Scalable parallel solvers for finite elements and isogeometric discretizations in computational cardiology

Luca F. Pavarino
Università di Milano, Italy

P. Colli Franzone, Università di Pavia, Italy
S. Scacchi, Università di Milano, Italy
S. Zampini, KAUST, Saudi Arabia

PETSc20
Argonne National Laboratory, June 15 - 18, 2015

Foreword

This talk will be on the use of PETSc in constructing and testing scalable domain decomposition solvers for cardiac reaction-diffusion models, from a user (not developer) perspective. Goal/hope is to show some of PETSc's greatest features applied to very challenging biomechanical applications:

- Modularity: PETSc helps greatly in experimenting with complex choices of proper submodels/solvers in order to balance biophysical accuracy vs. computational costs
- Depth of algorithmic options, in particular for KSP, PC, SNES
- Portability: thanks to PETSc our codes are not bound to machine turnover (HP Superdome, Compaq Alpha, IBM SP3, 4, 5, BG/Q, Cray XC40, + about 10 Linux Clusters ...)
- User support and documentation: always there and helpful

PETSc has also been essential in my teaching parallel computing classes and in advising PhD students

Introduction

We will focus on the first two of the three main cardiac functions:

- *bioelectrical: ionic currents through ionic channels of the cell membrane, excitation front generation and propagation of cardiac action potential in cardiac tissue*
- mechanical: contraction/relaxation of cardiac muscle
- haemodynamical: double pump $\rightarrow$ blood flow

Several large groups involved in cardiac modeling, e.g.:
U Auckland (IUPS Physiome Project), Johns Hopkins (CCBM), INRIA (euHeart, CardioSense3D), Oxford (Chaste, COR), Simula, EPFL/Mox/Emory (LifeV, MathCard),...

Large European effort in VPH Initiative (Virtual Physiological Human), FP7 ICT 2007.5.3, $\sim$ 72 M euro, www.vph-noe.eu/home
(1 NoE, 3 IPs, 9 STREPs, 2CAs) $\longrightarrow$ VPH Institute 2011 $\longrightarrow$ Horizon 2020?

P. Hunter, A. Quarteroni, ... *A vision and strategy for the virtual physiological human: a 2012 update*, Interface Focus 3(2), 2013

Coupled multiphysics in cardiac modeling

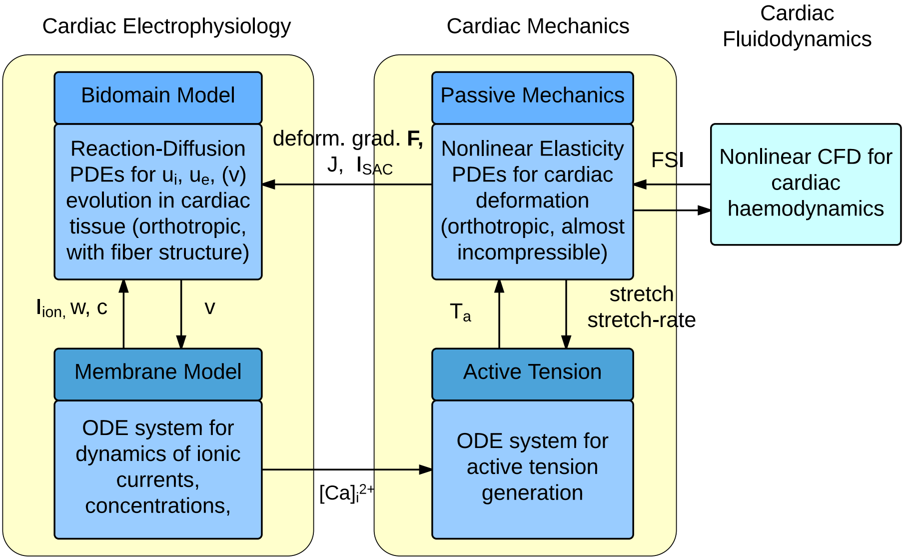

Reaction-Diffusion system of degenerate parabolic PDEs:

- Given $I_{app}^{i,e}$ (applied current), v_0, w_0 (initial conditions)
- find u_i, u_e =intra and extracellular potentials, (and $v = u_i - u_e$ = transmembrane potential), w =gating variables and c =ion concentrations such that:

Bidomain system (P-P formulation):

$$\chi C_m \frac{\partial v}{\partial t} - \mathrm{div}(D_i \nabla u_i) + \chi I_{ion}(v, w, c) = -I_{app}^i \qquad \text{in } \Omega \times (0, T)$$

$$-\chi C_m \frac{\partial v}{\partial t} - \mathrm{div}(D_e \nabla u_e) - \chi I_{ion}(v, w, c) = I_{app}^e \qquad \text{in } \Omega \times (0, T)$$

$$\frac{\partial w}{\partial t} = R(v, w), \qquad \frac{\partial c}{\partial t} = S(v, w, c) \qquad \text{in } \Omega \times (0, T)$$

with 0 Neumann b.c. for u_i, u_e, initial conditions for v, w, c
χ = ratio membrane area/tissue volume, C_m = surface capacitance

Conductivity tensors:

$$D_{i,e}(\mathbf{x}) = \sigma_l^{i,e}\ \mathbf{a}_l\mathbf{a}_l^T + \sigma_n^{i,e}\ \mathbf{a}_n\mathbf{a}_n^T + \sigma_t^{i,e}\ \mathbf{a}_t\mathbf{a}_t^T$$

$\sigma_l^{i,e}, \quad \sigma_n^{i,e}, \quad \sigma_t^{i,e} \;=$ conductivity coefficients along directions

$\mathbf{a}_l$: along fiber, $\mathbf{a}_n$: normal to lamina, $\mathbf{a}_t =$ tangent to lamina

$\Rightarrow$ electrical conductivity depends on fiber and laminar structure

1.2 Ionic model (Hodgkin - Huxley formalism, Nobel '63):

Ionic current I_{ion} and functions R, S in ODE systems are given by the chosen ionic membrane model:

- LR1, LRd00, LRd07, ... (ventricular, guinea pig)
- Shannon04, Mahajan07, ... (ventricular, rabbit)
- Ten Tusscher04, O'Hara-Rudy11, ... (ventricular, human)

Colli Franzone, LFP, Scacchi, Mathematical Cardiac Electrophysiology, Springer, 2014

Cardiac tissue modeled as a nonlinear elastic material. Notations:

- $\mathbf{X} = (X_1, X_2, X_3)^T \in \widehat{\Omega}$ undeformed cardiac domain
- $\mathbf{x} = (x_1, x_2, x_3)^T \in \Omega$ deformed cardiac domain
- $\mathbf{F}(\mathbf{X}, t) = \{F_{ij} = \frac{\partial x_i}{\partial X_j} \quad i, j = 1, 2, 3\}$ deformation gradient tensor and $J(\mathbf{X}, t) = det(\mathbf{F}(\mathbf{X}, t))$
- $\mathbf{C} = \mathbf{F}^T\mathbf{F}$ Cauchy-Green deformation tensor
- $\mathbf{E} = \frac{1}{2}(\mathbf{C} - \mathbf{I})$ Lagrange-Green strain tensor ($\mathbf{I}$ identity)
- $\mathrm{Div}, \mathrm{div}$ (Grad, ∇) the material, spatial divergence (gradient)

Equilibrium equations

deformed body	undeformed body
$\mathrm{div}\ \boldsymbol{\sigma} = 0, \qquad \mathbf{x} \in \Omega,$	$\mathrm{Div}(\mathbf{FS}) = 0 \qquad \mathbf{X} \in \widehat{\Omega},$

with $\mathbf{S} = \{S_{ij}\} = J\mathbf{F}^{-1}\boldsymbol{\sigma}\mathbf{F}^{-T}$ = 2nd Piola-Kirchhoff stress tensor

The stress tensor: passive and active components

a) Active stress assumption: $\mathbf{S}$ is the sum of

- an active biochemically generated component $\mathbf{S}^{act}$,
- a passive elastic component $\mathbf{S}^{pas}$,
- a volume component $\mathbf{S}^{vol}$,

$$\mathbf{S} = \mathbf{S}^{act} + \mathbf{S}^{pas} + \mathbf{S}^{vol}$$

Most used in the literature: Nash and Hunter 2000, Vetter and McCulloch 2000; Kerckhoffs et al. 2003; Nash and Panfilov 2004; Sainte-Marie 2006; Pathmanathan and Whiteley 2009; Gotkepe and Kuhl 2010; Jie, Gurev and Trayanova 2010; Niederer, Nash, Hunter, Smith 2011; ...

b) Active strain alternative assumption: multiplicative strategy for combining the passive $\mathbf{S}^{pas}$ and active $\mathbf{S}^{act}$ components,
Cherubini et al 2008, then used by Ambrosi et al. 2011, Nobile, Quarteroni and Ruiz-Baier 2012, Rossi et al. 2012...

canine biventricular geometry from Ayache et al. 2007,
orthotropic constitutive law from Holzapfel & Ogden 2009

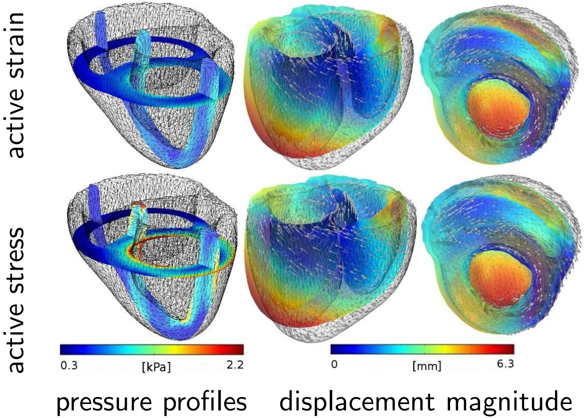

Rossi, Ruiz-Baier, LFP, Quarteroni, *IJNMBE* 28, 2012

Passive component $\mathbf{S}^{pas}$ given by suitable strain energy function W

$$S_{ij}^{pas} = \frac{1}{2}\left(\frac{\partial W}{\partial E_{ij}} + \frac{\partial W}{\partial E_{ji}}\right) \qquad i,j = 1,2,3.$$

We choose to model the myocardium as an orthotropic hyperelastic material, with the exponential strain energy function (see Eriksson et al. 2013)

$$W = \frac{a}{2b}\left(e^{b(\mathbf{I}_1-3)} - 1\right) + \sum_{i=l,t}\frac{a_i}{2b_i}\left(e^{b_i(\mathbf{I}_{4i}-1)^2} - 1\right) + \frac{a_{lt}}{2b_{lt}}\left(e^{b_{lt}\mathbf{I}_{8lt}^2} - 1\right),$$

$a,\ b,\ a_{(l,t,lt)},\ b_{(l,t,lt)}$ are positive material parameters,

$$\mathbf{I}_1 = tr(\mathbf{C}), \quad \mathbf{I}_{4l} = \widehat{\mathbf{a}}_l^T \mathbf{C}\, \widehat{\mathbf{a}}_l, \quad \mathbf{I}_{4t} = \widehat{\mathbf{a}}_t^T \mathbf{C}\, \widehat{\mathbf{a}}_t, \quad \mathbf{I}_{8lt} = \widehat{\mathbf{a}}_l^T \mathbf{C}\, \widehat{\mathbf{a}}_t,$$

$\widehat{\mathbf{a}}_{l,t}$ are the directions along and across fiber

Almost-incompressibility constraint and active component

Almost-incompressibility of myocardium enforced by adding to the strain energy a bulk modulus K times a volume change penalization term

$$W^{vol} = K\left(\sqrt{\det(\mathbf{C})} - 1\right)^2.$$

We assume the active component $\mathbf{S}^{act}$, acting only in the direction of the fiber (Pathmanathan et al. 2009, Whiteley 2007, Goktepek et al. 2010)

$$\mathbf{S}^{act} = T_a \frac{\widehat{\mathbf{a}}_l\,\widehat{\mathbf{a}}_l^T}{\widehat{\mathbf{a}}_l^T\,\mathbf{C}\,\widehat{\mathbf{a}}_l},$$

where $\widehat{\mathbf{a}}_l$ is the local fiber direction and T_a is the active tension.

1.4 Models of active tension

a) $T_a = T_a(t, Ca_i)$ depends only on Ca_i

$$\frac{dT_a}{dt} = \epsilon(Ca_i)\ [\eta([Ca_i - Ca_i^{rest}) - T_a]$$

where $\epsilon(Ca_i) = \epsilon_0 + (\epsilon_\infty - \epsilon_0)\exp(-\exp(-\xi(Ca_i - Ca_i^{rest})))$

(Kuhl et al., PBMB 2012, smooth variant of Nash, Panfilov, IJNMBE 2004)

b) $T_a = T_a(Ca_i, \lambda)$ depends on Ca_i and fiber stretch $\lambda = \sqrt{\hat{\mathbf{a}}_l^T \mathbf{C} \hat{\mathbf{a}}_l}$

$$T_a = \frac{Ca_i^n}{Ca_i^n + C_{50}^n}\ T_a^{max}(1 + \eta(\lambda - 1))$$

(Hunter et al. 1997)

c) $T_a = T_a\left(Ca_i, \lambda, \frac{d\lambda}{dt}\right)$ depends on Ca_i, stretch and stretch-rate

system of 4 ODEs (Land et al., J. Physiol, 2012)

The Bidomain model on the undeformed domain $\hat{\Omega}$

P-P formulation

$$\begin{cases} \chi\left(C_m \frac{\partial v}{\partial t} + I_{ion}^{me}\right) - \frac{1}{J}\mathrm{Div}\left(J\,\mathbf{F}^{-1} D_i \mathbf{F}^{-T} \mathrm{Grad}\, u_i\right) = 0 \\ -\chi\left(C_m \frac{\partial v}{\partial t} + I_{ion}^{me}\right) - \frac{1}{J}\mathrm{Div}\left(J\,\mathbf{F}^{-1} D_e \mathbf{F}^{-T} \mathrm{Grad}\, u_e\right) = I_{app}^{e} \\ \frac{\partial w}{\partial t} = R(v, w), \ \frac{\partial c}{\partial t} = S(v, w, c), \end{cases}$$

Mechano-electric feedback: deformation affects bioelectric phenomena, mostly during the repolarization phase.

- Conductivity coefficients modified with deformation gradient tensor $\mathbf{F}(\mathbf{X}, t)$ and $J(\mathbf{X}, t)$
- ionic term $I_{ion}^{me}(v, w, c, \lambda) = I_{ion} + I_{SAC}$ augmented with the stretch-activated current $I_{SAC}(v, \lambda)$
- possible presence of a convective term dependent on the velocity field $\mathbf{V} = \frac{\partial \mathbf{x}(\mathbf{X},\mathbf{t})}{\partial \mathbf{t}}$ of the deformation field.

2. Numerical methods in space and time

$\mathbf{Q}^1$ isoparametric FEM in space,
structured meshes based on PETSc DMDA objects

Splitting and IMEX method in time: given v^n, w^n, c^n, $\mathbf{x}^n$, $\mathbf{F}^n$,

a. Solve the membrane model with a first order IMEX method

to compute the new w^{n+1}, c^{n+1}, in particular Ca_i^{n+1}

b. Solve the coupled active tension and mechanical models

to compute new deformed coordinates $\mathbf{x}^{n+1}$, providing the new deformation gradient tensor $\mathbf{F}^{n+1}$ and active tension T_a^{n+1},

c. Solve the Bidomain system. Given w^{n+1}, c^{n+1}, $\mathbf{x}^{n+1}$, $\mathbf{F}^{n+1}$,

compute the new electric potentials u_i^{n+1}, u_e^{n+1},
$v^{n+1} = u_i^{n+1} - u_e^{n+1}$

Parallel Mechanical/Bidomain solvers at each time step

- mechanical nonlinear system:
  - outer iteration: Newton method
  - inner iteration (Jacobian system): GMRES, preconditioned by
  - preconditioner: Algebraic Multigrid (BoomerAMG from HYPRE) or BDDC (PCBDDC from PETSc)
- Bidomain system (linear because of IMEX decoupling):
  - Preconditioned Conjugate Gradient (PCG) method
  - preconditioner: Multilevel Hybrid Schwarz or PCBDDC
- Parallel libraries: mostly PETSc, + some MPI and HYPRE
- Computational platforms (thanks to PETSc portability):
  - local Linux clusters at Univ. of Milan/Pavia (small runs with $O(10^2)$ cores)
  - MIRA BG\Q at ANL, Fermi BG\Q at CINECA, Shaheen2 Cray XC40 at Kaust, Piz Dora Cray XC40 at CSCS

For DD overview see: A. Toselli and O. Widlund, *Domain Decomposition Methods: Theory and Algorithms*, Springer, 2005

- $\mathcal{T}_k$, $k = 0, ..., L-1$: nested triangulations of Ω, $\mathcal{T}_{L-1} = \mathcal{T}_h$

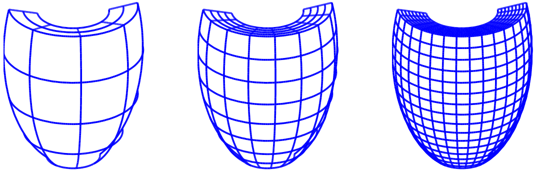

$\mathcal{T}_0 = 4 \cdot 4 \cdot 2$ $\qquad$ $\mathcal{T}_1 = 2\mathcal{T}_0$ $\qquad$ $\mathcal{T}_2 = 2\mathcal{T}_1 \cdots$

- $\mathcal{T}_k = \{\Omega_{km}\}_{m=1}^{N_k}$, subdomains with overlap δ_k and diameter H_k

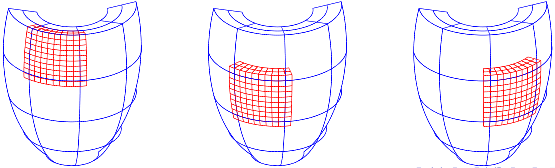

Matrix form of MAS(L) preconditioner $\mathcal{P}_{MAS}^{-1}$:

$$\mathcal{P}_{MAS}^{-1} = R_0^T B_0^{-1} R_0 + \sum_{k=1}^{L-1} \sum_{m=1}^{N_k} R_{km}^T B_{km}^{-1} R_{km}$$

- B_{km} = local bidomain matrix on Ω_{km} (level k, subdomain m)
- R_{km} = restriction matrix to nodes in Ω_{km}

- B_0 = coarse bidomain matrix on $\mathcal{T}_0$
- R_0 = restriction matrix to nodes in coarse mesh $\mathcal{T}_0$

Structured FEM and DD data management greatly simplified by using PETSc DMDA objects
(DMDACreate3d, DMCreateInterpolation, DMDAGetCorners,...)

Bidomain MAS preconditioners

Theorem: MAS(L) convergence rate bounds

The condition number of the Multilevel Additive Schwarz operator $\mathcal{P}_{MAS}^{-1}\mathcal{B}$ for the Bidomain system is bounded by

$$\boxed{\kappa_2(\mathcal{P}_{MAS}^{-1}\mathcal{B}) \leq C \max_{k=1,\dots,L-1} \left(1 + \frac{H_k}{\delta_k}\right)}$$

with C constant independent of:

$L =$ number of levels, $\delta_k =$ overlap at level k,

$h_k =$ mesh size on level k, $H_k (= h_{k-1})$ subdomain diam. at level k.

Proof + numerical results in

LFP, S. Scacchi, SIAM J. Sci. Comp., 31 (1), 2008

Analogous scalability bound holds for decoupled NKS MAS(2)

M. Munteanu, LFP, S. Scacchi, SIAM J. Sci. Comp., 31 (5), 2009

and for PE formulation with/without block-preconditioners

LFP, S. Scacchi, SIAM J. Sci. Comp., 33 (4), 2011

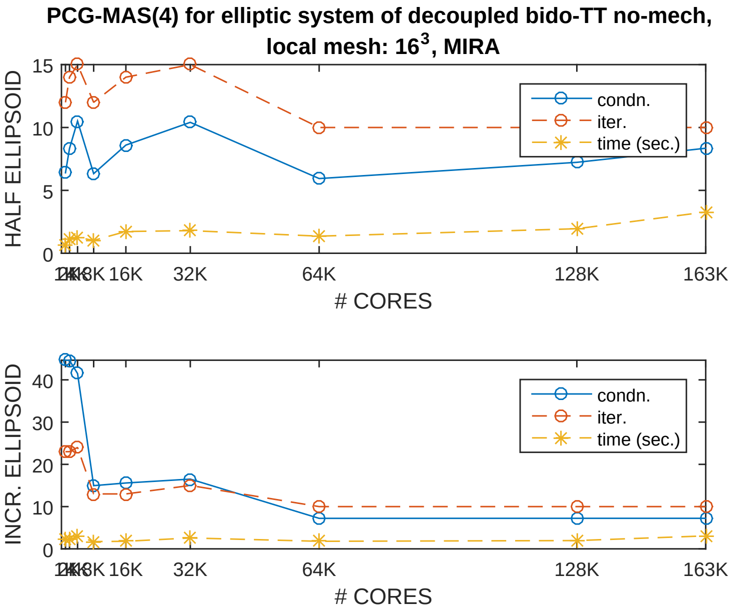
PCG-MAS(4) for elliptic system of decoupled bido-TT no-mech,
local mesh: 16^3, MIRA
HALF ELLIPSOID
CORES
1K 2K 4K 8K 16K 32K 64K 128K 163K
0 5 10 15
condn.
iter.
time (sec.)
INCR. ELLIPSOID
CORES
1K 2K 4K 8K 16K 32K 64K 128K 163K
0 10 20 30 40
condn.
iter.
time (sec.)

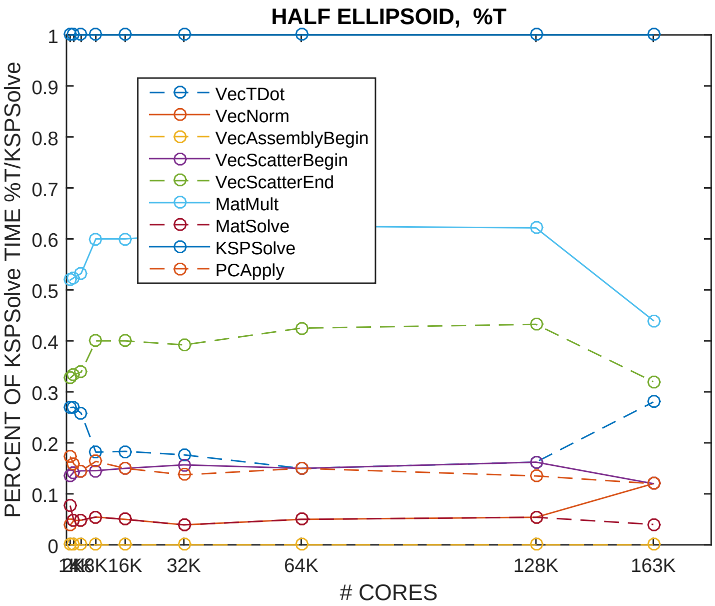
HALF ELLIPSOID, %T
PERCENT OF KSPSolve TIME %T/KSPSolve
1
0.9
0.8
0.7
0.6
0.5
0.4
0.3
0.2
0.1
0
VecTDot
VecNorm
VecAssemblyBegin
VecScatterBegin
VecScatterEnd
MatMult
MatSolve
KSPSolve
PCApply
16K
32K
64K
128K
163K
CORES

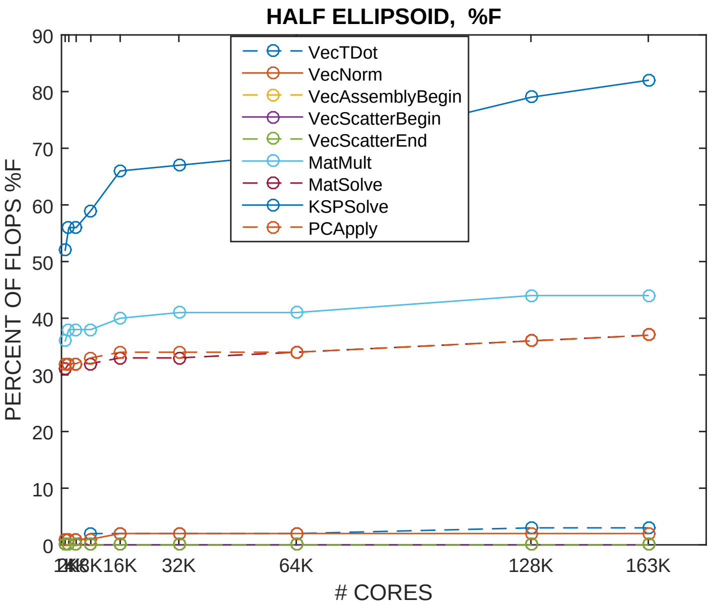
HALF ELLIPSOID, %F
VecTDot
VecNorm
VecAssemblyBegin
VecScatterBegin
VecScatterEnd
MatMult
MatSolve
KSPSolve
PCApply
PERCENT OF FLOPS %F
90
80
70
60
50
40
30
20
10
0
1K
2K
4K
8K
16K
32K
64K
128K
163K
CORES

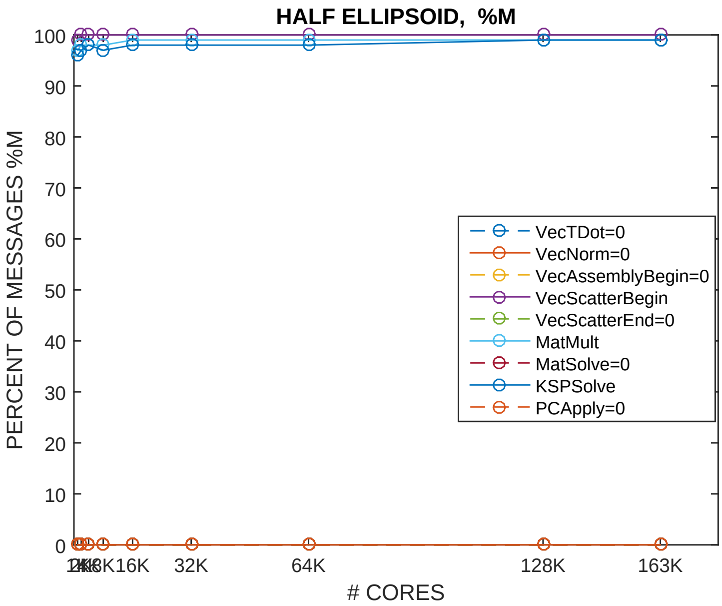
HALF ELLIPSOID, %M
PERCENT OF MESSAGES %M
100
90
80
70
60
50
40
30
20
10
0
16K
32K
64K
128K
163K
# CORES
VecTDot=0
VecNorm=0
VecAssemblyBegin=0
VecScatterBegin
VecScatterEnd=0
MatMult
MatSolve=0
KSPSolve
PCApply=0

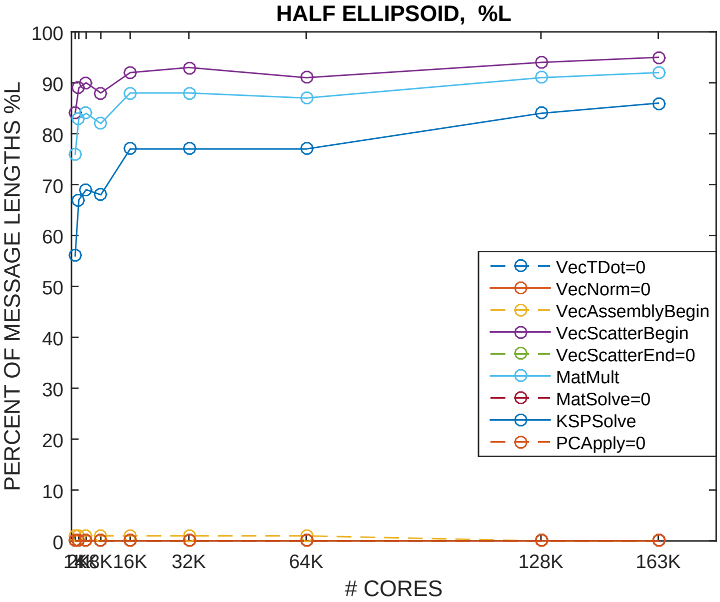
HALF ELLIPSOID, %L
PERCENT OF MESSAGE LENGTHS %L
100
90
80
70
60
50
40
30
20
10
0
1K
2K
4K
8K
16K
32K
64K
128K
163K
# CORES
VecTDot=0
VecNorm=0
VecAssemblyBegin
VecScatterBegin
VecScatterEnd=0
MatMult
MatSolve=0
KSPSolve
PCApply=0

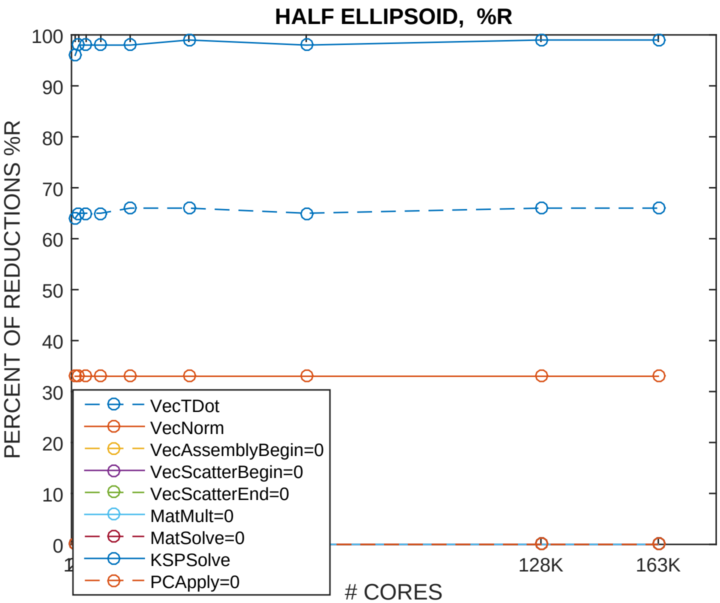
HALF ELLIPSOID, %R
PERCENT OF REDUCTIONS %R
100
90
80
70
60
50
40
30
20
10
0
128K
163K
CORES
VecTDot
VecNorm
VecAssemblyBegin=0
VecScatterBegin=0
VecScatterEnd=0
MatMult=0
MatSolve=0
KSPSolve
PCApply=0

Recent extension of 2-level MAS to Isogeometric Analisys (IGA) (L. Charawi PhD thesis, Univ of Milano, 2014 + DD22 Proc., to appear)

NURBS basis functions with $p = 3$, $k = 2$, $H/h = 4$

Bidomain weak scalability test:

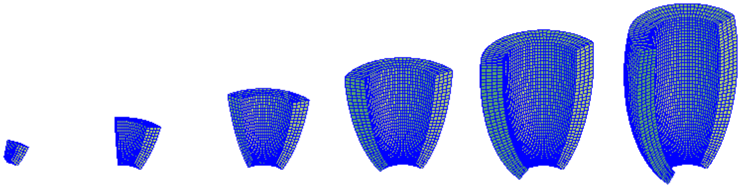

N	Unprec. it.	Unprec. k_2	1-level MAS it.	1-level MAS $\kappa_2 = \lambda_{max}/\lambda_{min}$	2-level MAS it.	2-level MAS $\kappa_2 = \lambda_{max}/\lambda_{min}$
$2\times 2\times 1$	765	2.8e4	14	10.3=4.0/3.9e-1	11	5.7=4.9/8.7e-1
$4\times 4\times 1$	1236	4.9e4	27	58.6=4.8/8.2e-2	10	6.6=5.1/7.6e-1
$6\times 6\times 1$	1539	7.3e4	35	1.4e2=4.9/3.4e-2	9	6.3=5.0/8.0e-1
$8\times 8\times 1$	1949	1.0e5	47	2.7e2=4.9/1.8e-2	8	5.5=4.9/8.9e-1
$10\times 10\times 1$	2180	1.1e5	55	4.5e2=8.0/1.1e-2	8	5.5=4.9/9.0e-1
$12\times 12\times 1$	2307	1.2e5	63	6.7e2=4.9/7.3e-3	8	5.5=4.9/9.0e-1

A) BNN (Balancing Neumann-Neumann) scaled speedup on slabs

$$S_{BNN}^{-1} = S_0 + (I - S_0 S)(\sum_{i=1}^{N} D_i^T S^{i^\dagger} D_i)(I - S S_0)$$

$S = B_{\Gamma\Gamma} - B_{I\Gamma}^T B_{II}^{-1} B_{I\Gamma}$ (Bidomain Schur compl.)

$$\mathcal{B} = \begin{bmatrix} B_{II} & B_{I\Gamma} \\ B_{I\Gamma}^T & B_{\Gamma\Gamma} \end{bmatrix}.$$

$S^{i^\dagger}$ = pseudoinverse of local Schur complement (Neumann solver on Ω_i)

S_0 = coarse solver, D_i = scaled restriction op.

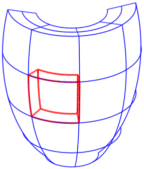

procs		Ω dofs	Γ dofs	it.	λ_{min}	λ_{max}	κ_2
16	(4x4x1)	235'225	14'325	14	1.00	5.08	5.08
64	(8x8x1)	931'225	66'325	15	1.00	5.75	5.75
144	(12x12x1)	2'088'025	155'925	16	1.00	5.91	5.91
256	(16x16x1)	3'705'625	283'125	16	1.00	5.84	5.84
400	(20x20x1)	5'784'025	447'925	16	1.00	5.93	5.93
576	(24x24x1)	8'323'225	650'325	16	1.00	5.99	5.99

B) BDDC (Balancing Domain Decomposition with Constraints) scaled speedup on slabs

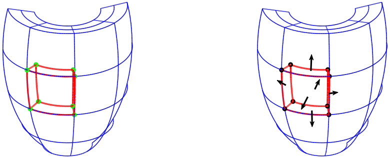

Coarse space $\widehat{W}_{\Pi}$: a: vertex + edge averages; b: vertex + edge aver + face aver.

procs		a: $\widehat{W}_{\Pi}$ dofs	iter	λ_{min}	λ_{max}	κ_2
16	(4x4x1)	222	12	1.00	3.33	3.33
64	(8x8x1)	910	13	1.00	3.51	3.51
144	(12x12x1)	2046	14	1.00	3.56	3.56
256	(16x16x1)	3630	14	1.00	3.59	3.59
400	(20x20x1)	5662	14	1.00	3.59	3.59
576	(24x24x1)	8141	14	1.00	3.60	3.60

BCX/5120 Cineca cluster (Zampini, Numer. Math. 2013 + M3AS 2014)

more recent results on FERMI BG/Q

weak scaling with local size $H/h = 20^3$
coarse problem solved by MUMPS Cholesky factorization

Uses Zampini's PETSc PCType PCBDDC and PCBDDCCreateFETIDPOperators

				BDDC		FETI-DP		
procs	$\lvert\widehat{W}\rvert$	$\lvert\widehat{W}_\Pi\rvert$	$\lvert\widehat{W}_\Gamma\rvert$	iter	time	$\lvert\Lambda\rvert$	iter	time
5^3	1.7M	1.3K	0.2M	21	0.28	0.2M	20	0.26
10^3	13M	9.6K	1.8M	22	0.30	2.0M	21	0.27
15^3	46.7M	30.8K	6.5M	22	0.36	7.1M	22	0.32
20^3	110.6M	70.9K	15.7M	23	0.40	17.1M	22	0.36
25^3	215.7M	135.9K	31.0M	23	0.53	33.8M	23	0.50
30^3	372.3M	231.8K	53.8M	23	0.81	58.8M	23	0.74

4.3 Mechanical solver: AMG weak scalability

- Simulation of 1.5 *ms* (30 time steps of $\tau = 0.05$ *ms*) during the plateau phase on truncated ellipsoidal domains.
- Fixed local mechanical dof per subdomain: 13 476

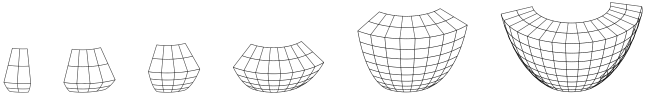

Mechanical solver - AMG preconditioner				
procs	dof	outer iter. Newton	inner iter. GMRES	CPU time
8	107 811	2	42	12.06
27	352 947	2	42	16.70
64	823 875	2	39	23.45
125	1 594 323	2	39	30.66
216	2 738 019	2	40	49.12
512	6 440 067	2	40	75.09

Mechanical solver: AMG strong scalability

Fixed global mechanical dof: 823 872

Mechanical solver - AMG preconditioner					
procs	local dof	nit	lit	time	speedup
8	102 984	2	41	110.84	-
16	51 492	2	40	63.61	1.74 (2)
32	25 746	2	41	34.64	3.20 (4)
64	12 873	2	39	23.26	4.76 (8)
128	6 436	2	40	16.08	6.89 (16)
256	3 218	2	40	15.50	7.15 (32)
512	1 609	2	41	16.97	6.53 (64)

nit = Newton iterations
it = CG iteration counts
time = CPU time in sec. to solve mechanical pb.

4.4 Bidomain - Multilevel Hybrid Schwarz weak scalability

Fixed local Bidomain dof per subdomain: 68 656

Bidomain solver - MHS(4) preconditioner							
		non-deforming ($\mathbf{C} = \mathbf{I}$)			deforming		
procs	dof	κ_2	it	time	κ_2	it	time
8	549 250	1.11	3	1.05	1.11	3	1.31
27	1 825 346	1.11	3	1.19	1.12	3	1.17
64	4 293 378	1.12	3	1.23	1.13	3	1.21
125	8 346 562	1.13	3	1.31	1.18	4	1.49
216	14 378 114	1.18	4	1.55	1.20	4	1.55
343	22 781 250	1.15	4	1.62	1.17	4	1.66
512	33 949 186	1.14	4	1.96	1.17	4	1.67

κ_2 = average condition number per time step

it = average CG iteration counts per time step

time = average CPU time in seconds to solve one Bidomain linear system

Bidomain - Multilevel Hybrid Schwarz strong scalability

Fixed global Bidomain dof: 4 293 376

Bidomain solver - MHS(4) preconditioner					
procs	local dof	κ_2	it	time	speedup
8	536 672	1.13	3	9.18	-
16	268 336	1.13	3	5.16	1.78 (2)
32	134 168	1.14	3	2.62	3.50 (4)
64	67 084	1.15	3	1.30	7.06 (8)
128	33 542	1.16	4	0.72	12.75 (16)
256	16 771	1.19	4	0.48	19.12 (32)
512	8 385	1.20	4	0.26	35.31 (64)

4.5 Whole heartbeat: ventricular wedge deformation + v

4.5 Whole heartbeat: ventricular wedge deformation + v

endo

4.5 Whole heartbeat: ventricular wedge deformation + v

endo

transmural

Whole heartbeat

Simulation of 500 ms on a truncated half ellipsoidal domain modeling half left ventricle. Number of processors = 24

Mechanical Solver: dof = 32967, time step = 0.25 ms

Prec.	*Newton nit*	*Total nit*	*GMRES it*	*Total it*	*time cpu*	*Tot cpu*
AMG	3	7031	796	6.5 ML	28.42s	15h 47m

Bidomain solver: dof = 9 655490, time step = 0.05 ms

Prec.	κ_2	CG_{it}	$Total_{it}$	$time_{cpu}$	$Total_{cpu}$
MAS(4)	6.18	8	81 178	1.54s	4h 16m

κ_2: average condition number per time step

P. Colli Franzone, LFP, S. Scacchi, Appl. Numer. Math, 2015

Land - Niederer et al. active tension model
Fixed global mesh on ellipsoidal domain: $769 \times 769 \times 97$
3-level BDDC code by S. Zampini

	V			VE			VEF		
procs	nit	lit	time	nit	lit	time	nit	lit	time
512	3	353	31.1	3	144	21.4	3	143	22.1
1024	3	317	12.8	3	132	9.4	3	127	9.9
2048	3	464	9.5	3	196	8.1	3	189	10.2
4096	3	341	5.6	3	163	5.5	3	158	7.4
8192	3	279	6.3	3	141	6.9	3	166	8.1

Shaheen 2 (KAUST)
/medskip
LFP, S. Scacchi, S. Zampini, submitted, 2015

Mechanical solver: 2-level BDDC weak scalability

Shaheen2 (KAUST)
Passive model by Vetter & M, active model by Goktepe et al.
local mesh 20^3 (electrical), 5^3 (mechanical), global size increases with core count,
nit $\approx 4 - 40$ (not reported)

	Slab domains						Ellipsoidal domains					
	V		VE		VEF		V		VE		VEF	
procs	lit	time	lit	time	lit	time	lit	time	lit	time	lit	time
256	96	0.3	41	0.4	37	0.4	473	0.7	165	0.9	150	0.8
512	93	0.4	40	0.4	37	0.5	566	1.5	185	1.0	163	1.1
1024	90	0.5	38	0.6	34	0.6	598	2.1	177	1.6	153	1.7
2048	96	0.7	38	0.7	34	0.9	644	3.1	180	2.1	158	2.6
4096	88	0.9	38	1.1	29	1.3	589	5.0	181	3.4	154	4.2
8192	89	1.5	36	1.9	29	2.7	626	28.3	192	6.5	167	7.9
16384	88	2.4	33	3.4	26	5.4	796	33.2	189	11.2	148	14.1

V = Vertex, E = Edges averages, F = Faces averages

Whole beat: mechanical BDDC with Land-Niederer T_a

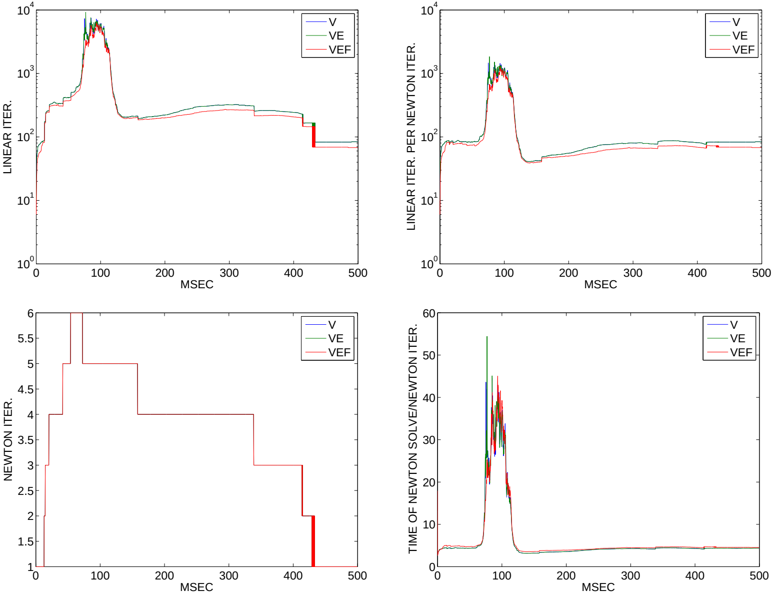

5. Applications: epicardial APD distributions

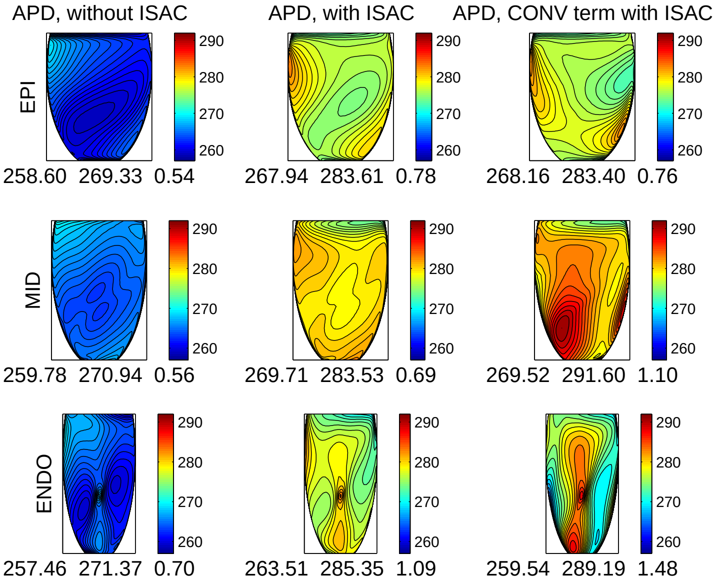

Transmural APD distributions

without ISAC | with ISAC

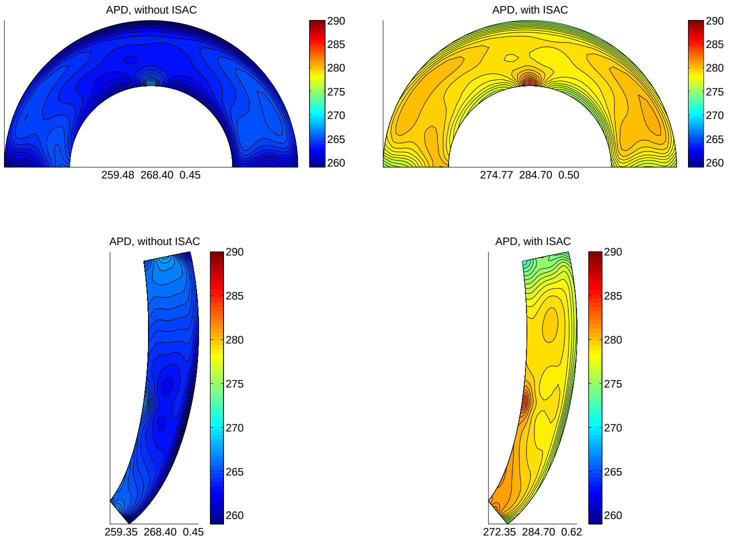

Conclusions

- Large-scale 3D cardiac simulations now possible due to advances in parallel architectures, libraries (PETSc), solvers
- Scalable and efficient DD solvers (multilevel Schwarz, BDDC,...) available for both:
  - Bidomain model (IMEX linearization) and
  - cardiac electromechanical models with orthotropic strain energy functions.

  Mechanical solvers (Newton-Krylov) using AMG not quite scalable, better performance with DD preconditioners

PETSc modularity helps greatly in experimenting with complex choices of proper submodels/solvers to balance biophysical accuracy vs. computational costs: ionic model, calcium dynamics, Bidomain/Monodomain, active tension, mechanical constitutive law.

PETSc has been essential in my professional work, in advising PhD students, in teaching parallel computing classes

Current/future work

- extend multilevel DD solvers to anatomic cardiac geometries:
  - unstructured meshes (go from DMDA to IS PETSc objects),
  - isogeometric analysis (via PetIGA library)
- explore other nonlinear solvers (nonlinear Schwarz, FAS, ...)
- explore better coupling/decoupling strategy of submodels in order to increase numerical stability/efficiency
- continue advanced Bidomain simulations: reentry genesis/termination, virtual electrode polarization, shock waveform (mono/biphasic) and energy optimization,...
- add coupling with haemodynamical models

Many thanks to Barry and the PETSc Team for this great library:
Happy 20th Birthday and many more!

THANK YOU

New book from Springer

Volume 13

Mathematical Cardiac Electrophysiology

Piero Colli Franzone, Luca F. Pavarino, Simone Scacchi

This book covers the main mathematical and numerical models in computational electrocardiology, ranging from microscopic membrane models of cardiac ionic channels to macroscopic bidomain, monodomain, eikonal models and cardiac source representations. These advanced multiscale and nonlinear models describe the cardiac bioelectrical activity from the cell level to the body surface and are employed in both the direct and inverse problems of electrocardiology.

The book also covers advanced numerical techniques needed to eff ciently carry out large-scale cardiac simulations, including time and space discretizations, decoupling and operator splitting techniques, parallel f nite element solvers. These techniques are employed in 3D cardiac simulations illustrating the excitation mechanisms, the anisotropic effects on excitation and repolarization wavefronts, the morphology of electrograms in normal and pathological tissue and some reentry phenomena.

The overall aim of the book is to present rigorously the mathematical and numerical foundations of computational electrocardiology, illustrating the current research developments in this fast-growing f eld lying at the intersection of mathematical physiology, bioengineering and computational biomedicine. This book is addressed to graduate student and researchers in the f eld of applied mathematics, scientif c computing, bioengineering, electrophysiology and cardiology.

MS&A

Series Editors:

Alfio Quarteroni (*Editor-in-Chief*) • Tom Hou • Claude Le Bris • Anthony T. Patera • Enrique Zuazua

MS&A publishes advanced textbooks and research-level monographs that will illustrate the scientific foundations of the modeling and simulation process as well as concrete instances of its role in addressing complex and relevant problems in everyday life.
Mathematical modeling aims to describe through mathematics the different aspects of the real world, their dynamics and their interaction. Numerical simulation provides accurate and certified solutions to complex mathematical models by means of scientific computing. Modeling and numerical simulation have become the road-map for mathematics to develop and analyze novel techniques to solve problems in basic sciences (such as physics, chemistry, biology) and engineering, environmental, life and social sciences.
The purpose of this series is to host high level contributions describing the interplay among mathematical analysis, numerical analysis and scientific computing, advanced programming techniques, control and optimization, validation, verification and testing. This interplay makes the modeling and numerical simulation process as a whole a unique and effective tool for applied sciences as well as for enhancing technological innovation.

Mathematics

ISBN 978-3-319-04800-0

springer.com

Volume 13 • MS&A **Mathematical Cardiac Electrophysiology • P. Colli Franzone, L.F. Pavarino, S. Scacchi**

AB

Volume 13

Mathematical Cardiac Electrophysiology

Piero Colli Franzone • Luca F. Pavarino • Simone Scacchi

MS&A

Modeling, Simulation & Applications

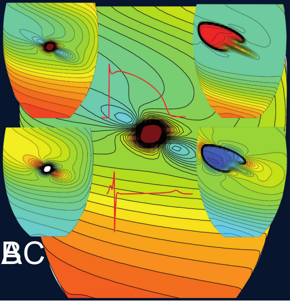

BC